

**Title:** A multifunctional role of Leucine-rich-alpha 2 glycoprotein 1 in cutaneous wound healing under normal and diabetic conditions

**Authors:** Chenghao Liu <sup>1</sup>, Melissa Hui Yen Teo <sup>2</sup>, Sharon Li Ting Pek <sup>3</sup>, Mei Ling Leong <sup>4</sup>, Hui Min Tay <sup>1,5</sup>, Han Wei Hou<sup>1,5</sup>, Ruedl Christiane <sup>4</sup>, Subramaniam Tavintharan <sup>3,6,7</sup>, Wanjin Hong <sup>2\*</sup>, Xiaomeng Wang <sup>1,2,8\*</sup>

**Affiliations:**

1. Lee Kong Chian School of Medicine, Nanyang Technological University, Singapore
2. Institute of Molecular and Cell Biology, Proteos, Agency for Science, Technology and Research, Singapore
3. Clinical Research Unit, Khoo Teck Puat Hospital, Singapore
4. School of Biological Sciences, Nanyang Technological University, Singapore
5. School of Mechanical and Aerospace Engineering, Nanyang Technological University, Singapore
6. Diabetes Centre, Admiralty Medical Centre, Singapore
7. Department of Medicine, Division of Endocrinology, Khoo Teck Puat Hospital, Singapore
8. Singapore Eye Research Institute, The Academia, Singapore

**\*Corresponding authors:** Xiaomeng Wang (Email: wangxiaomeng@ntu.edu.sg; address: Lee Kong Chian School of Medicine, Nanyang Technological University, Singapore), Wanjin Hong (Email: mcbhwj@imcb.a-star.edu.sg; address: Institute of Molecular and Cell Biology, 61 Biopolis Drive, Proteos, Agency for Science Technology & Research, Singapore),

## **Abstract**

Delayed wound healing is commonly associated with diabetes. It may lead to amputation and death if not treated timely. Limited treatments are available partially due to the limited understanding of the complex disease pathophysiology. In this study, we investigated the role of Leucine-rich alpha-2-glycoprotein 1 (LRG1) in normal and diabetic wound healing. Firstly, our data showed that LRG1 was significantly increased at the inflammation stage of murine wound healing, and bone marrow-derived cells served as a major source of LRG1. Deletion of LRG1 causes impaired immune cell infiltration, re-epithelialization and angiogenesis. As a consequence, there is a significant delay in wound closure. On the other hand, LRG1 was markedly induced in diabetic wounds in both humans and mice. LRG1-deficient mice were resistant to diabetes-induced delay in wound repair. We further demonstrated that this could be explained by the mitigation of increased neutrophil extracellular traps (NETs) in diabetic wounds. Mechanistically, LRG1 mediates NETosis in an Akt-dependent manner through TGF-beta type I receptor kinase ALK5. Taken together, our studies demonstrate that LRG1 derived from bone marrow cells is required for normal wound healing, but excess LRG1 expression in diabetes contributes to chronic wounds.

## **Introduction**

Wound healing is a natural reparative response to tissue injury. It proceeds through four continuous and overlapping phases: homeostasis, inflammation, proliferation and tissue remodeling (1). Failure to progress through these phases in an orderly manner leads to impaired wound healing, which represents one of the common causes of morbidity associated with diabetes, affecting approximately 25% of individuals with diabetes (2). These wounds frequently serve as portals of entry for bacterial infection that may lead to sepsis and lower-extremity amputation (3). Staggeringly, patients with lower-extremity amputation have a 5-year mortality rate of up to 50% (4). With the rising prevalence of diabetes, the incidence of wound complications is expected to increase substantially, posing a significant socioeconomic burden (5).

A plethora of factors contribute to delayed wound closure in diabetic patients, such as excessive neutrophil infiltration and activation, impaired angiogenesis, and defective epithelial cell migration and proliferation (6). These defects lock the wound into a self-perpetuating inflammatory stage (7), which causes further tissue injury by increasing the production of inflammatory cytokines, reactive oxygen species (ROS), destructive enzymes and cytotoxic extracellular traps in a process termed NETosis (8). Thus, targeting inflammation serves as an attractive strategy to kick-start the proliferation phase of wound healing and promote repair. A number of anti-inflammatory agents have been developed over the last 20 years (9). Despite being effective in promoting wound closure in rodent models, limited success has been achieved in clinical trials (10). This is likely due to the highly dynamic and complex interactions between different types of cell, extracellular matrix (ECM) components, and soluble factors present in the wound microenvironment. A better understanding of the molecular mechanisms underlying diabetes-associated healing deficiency will guide the

development of more effective therapeutics to treat wounds that do not respond sufficiently to good standard care.

Leucine-rich-alpha-2 glycoprotein 1 (LRG1) is a secreted glycoprotein that was previously reported to regulate pathological neovascularization in the eye by switching the angiostatic TGF $\beta$ 1-Smad2/3 signaling towards the pro-angiogenic TGF $\beta$ 1-Smad1/5/8 signaling in endothelial cells (11). Besides its role in ocular angiogenesis, LRG1 is intimately associated with many inflammatory and autoimmune conditions (12-15) and tumour malignancy (16-19), which shares fundamental molecular mechanisms with chronic wound healing. Recently, elevated serum LRG1 levels were reported in diabetic patients with peripheral arterial disease (20), a major risk factor for diabetic foot ulcers (DFU) (21). Paradoxically, exogenous LRG1 was reported to accelerate wound healing by promoting keratinocyte migration in animal models (22).

Here, *Lrg1*-null mice were used to better understand the role of LRG1 in normal and diabetic wound healing. This study demonstrated, for the first time, that infiltrating leukocytes serve as a major source of LRG1 and contribute to the transient elevation of LRG1 levels at the inflammatory phase of normal wound healing. Deletion of LRG1 leads to a significant delay in wound closure under normal condition due to an impaired inflammatory response, re-epithelialization, and angiogenesis in the wound bed. On the other hand, elevated LRG1 expression was observed in plasma and wound tissue of human DFU patients and mice with Streptozotocin (STZ)-induced type I diabetes, possibly due to increased neutrophil infiltration (23), while *Lrg1*<sup>-/-</sup> mice are resistant to diabetes-induced delay in wound closure, which is accompanied with reduced NET formation. Together, this study revealed an essential role of LRG1 in cutaneous wound healing under normal and diabetic conditions. An orchestrated regulation of LRG1 expression is critical for efficient wound closure.

## **Research Design and Methods**

### **Human Sample Analysis**

This study was approved by Khoo Teck Puat Hospital Ethics Review Board (NHG Domain Specific Review Board). Adults between 21- 90 years old, with Type 2 Diabetes (T2D) seen in Diabetes Centre of Khoo Teck Puat Hospital (Singapore) were enrolled into this study. Fasting blood and debrided tissues were collected from patients with ulcers during their podiatry assessment clinic. Fasting blood samples were centrifuged within 1 hour after collection and kept at 4°C during this period. Thereafter, they were stored at -80°C in aliquots and used without additional freeze-thaw cycles. Devitalized tissue obtained from desloughing and debridement performed as part of their usual care. These samples were stored in liquid nitrogen until retrieved for assays described below. Control samples were obtained from non-T2D patients with venous ulcers in the same clinic. Serum level of LRG1 was measured using an ELISA kit (Immuno-Biological Laboratories, Germany) according to manufacturer's instructions.

### **Animals and induction of type I diabetes**

C75BL/6J mice were purchased from InVivos (Singapore). *Lrg1*<sup>-/-</sup> mice were originally generated by the University of California Davies knockout mouse project (KOMP) repository (<http://www.komp.org>) and were a generous gift from J Greenwood (UCL Institute of Ophthalmology). Animal experiments were performed in compliance with the guidelines of the Institutional Animal Care and Use Committee (ARF-SBS/NIE-A0268/A19036) of Nanyang Technological University Singapore and the Guide for Care and Use of Laboratory Animals published by US National Institutes of Health. Type I diabetes was induced in 6-8 week old male mice by i.p. injection of 50 mg/kg STZ (50 mM sodium citrate buffer, pH 4.5) for five consecutive days as described (24). Diabetes was confirmed when Fasting Blood Glucose (FBG) was higher than 200mg/dl.

### **Creation of full thickness cutaneous wounds**

Six full-thickness cutaneous wounds were created on mouse dorsal skin using 4-mm Integra™ Miltex™ Standard Biopsy Punches (Thermo Fisher Scientific, USA). Wounds were imaged daily using a digital camera. Wound size was quantified using Image J (National Institutes of Health, USA). 6-mm Integra™ Miltex™ Standard Biopsy Punches (Thermo Fisher Scientific, USA) were used for biopsy collection at different time points following injury.

### **Bone marrow transplantation**

Six-week old mice were irradiated at two doses of 5.5 Gy irradiation using a BioBeam gamma irradiation device (Gamma Service Medical, Germany). Bone marrow cells (BMCs) from female mice were harvested and filtrated through a 70µm cell strainer (Falcon).  $3 \times 10^6$  bone marrow cells were intravenously injected into the irradiated recipient mice through the tail vein 24 hours after the irradiation. Eight weeks after reconstitution, wounds were created at flanks of recipient mice.

### **Cells and cell culture**

Primary mouse and human peripheral blood neutrophils (Institutional Review Board of Nanyang Technological University, IRB-2014-04/27) were isolated, purified and cultured as previously described (25, 26). Human neutrophil-like cells (dHL-60) were derived from human promyelocytic leukemia cell line (HL-60, ATCC) by incubating with 1% dimethyl sulfoxide (DMSO, Sigma) for 7 days. Human dermal microvascular endothelial cells (HDMECs, Promocell, USA), human keratinocyte line HaCaT (ATCC, USA) and Freestyle 293-F cells (Gibco, Thermo Fisher Scientific) were maintained according to supplier's instruction. Cells were treated with  $20 \mu\text{g ml}^{-1}$  recombinant human LRG1 (rhLRG1), LDN193189 (Sigma, 100 nM), SB431542 (Sigma, 10µM) and MK-2206 (Selleck, 10µM) and as indicated.

## Statistical analysis

Data are represented as mean  $\pm$  s.e.m. Statistical analyses were performed using unpaired, two-tailed Student's t-test or one-way/two-way ANOVA followed by Tukey/Bonferroni post-test analysis using Prism 5 (GraphPAD Software Inc.). \*P < 0.05; \*\*P < 0.01; \*\*\*P < 0.001.

All other methods are described in the Supplement Information.

## Results

### **LRG1 is produced by wound-infiltrating bone marrow-derived cells following injury**

To address the role of LRG1 in wound healing, the expression of LRG1 was examined in normal C56BL/6 mouse skin tissues by immunohistochemistry and revealed a very weak staining in the dermis (Figure 1A). Western blot was used to evaluate LRG1 expression in wound tissues at various time points following injury (Figure 1B). Our data showed that LRG1 was increased as early as six hours post-injury and reached its highest level 24 hours after wounding. LRG1 level then declined gradually and went back to basal level on day-five following injury. It is worth noting that LRG1 expression in surrounding intact skin tissues remained low throughout the wound healing process (Figure S1).

Immunofluorescence staining was used to identify the source of LRG1 during wound healing. We found that *Lrg1*<sup>+</sup> cells were mainly present in the provisional matrix and were co-localized with CD11b<sup>+</sup> myeloid cells in day-one wound tissues (Figure 1C). To confirm this observation, allogenic bone marrow transplantation (BMT) study was carried out in irradiated wild-type mice using BMCs from *Lrg1*<sup>-/-</sup> mice and wild-type littermate controls. Similar to what we observed in unirradiated C56BL/6 mice, quantitative RT-PCR showed that *Lrg1* transcript was significantly higher in day-one wound tissues of wild-type mice transplanted with wild-type BMCs, whereas *Lrg1* was not induced in those that received *Lrg1*<sup>-/-</sup> BMCs (Figure 1D). These data suggest that wound infiltrating bone marrow-derived cells (BMDCs) serve as a major source of LRG1 during cutaneous wound healing.

### **LRG1 is critical for timely wound closure**

To elucidate the functional role of LRG1 in cutaneous wound healing, 4-mm full-thickness wounds were created on the dorsal skin of wild-type and *Lrg1*<sup>-/-</sup> mice. *Lrg1*<sup>-/-</sup> mice demonstrated a significant delay in wound closure as compared to wild-type controls (Figure 2A). As LRG1 is remarkably induced at the inflammatory phase of wound healing, the number of wound infiltrating immune cells were analyzed in the wound bed of wild-type and *Lrg1*<sup>-/-</sup> mice. Neutrophils are the first inflammatory cells to be recruited to the wound bed (27). After performing their functions, apoptotic neutrophils and tissue debris are cleared by macrophages, which eventually lead to the resolution of inflammation (28). Immunofluorescence staining showed a significant reduction in the number of wound infiltrating MPO<sup>+</sup> neutrophils (Figure 2B) and F4/80<sup>+</sup> macrophages (Figure 2C) one day and five-day post-injury respectively. As BMDCs are major LRG1-producing cells, we next performed BMT between *Lrg1*<sup>-/-</sup> mice and wild-type controls. Irradiated *Lrg1*<sup>-/-</sup> mice and wild-type control mice were intravenously transplanted with wild-type or *Lrg1*<sup>-/-</sup> BMCs (Figure 2D). Consistent with what was observed in unirradiated control mice, wound closure was significantly delayed in *Lrg1*<sup>-/-</sup> recipients transplanted with *Lrg1*<sup>-/-</sup> BMCs as compared to that in wild-type recipients transplanted with wild-type BMCs. On the other hand, wound closure in wild-type recipients transplanted with *Lrg1*<sup>-/-</sup> BMCs was delayed substantially, whereas wild-type BMCs fully rescued the delayed wound healing in *Lrg1*<sup>-/-</sup> mice. Together, these data provide compelling evidence that LRG1-producing BMDCs are critical for timely wound closure.

### **LRG1 promotes neutrophil adhesion via inducing the expression of L-selectin**

The ability of neutrophils to adhere to the endothelium is critical for their recruitment to the wound bed (29). To understand LRG1's role in neutrophil infiltration, we investigated the ability of dHL-60 cells to adhere to a HDMEC monolayer in the presence and absence of rhLRG1. Our study showed that rhLRG1 significantly promoted dHL-60 cell adhesion to the

HDMEC monolayer (Figure 3A). Conversely, dHL-60 cells subjected to siRNA-mediated LRG1 knockdown were less responsive to TNF $\alpha$ -induced adhesion to HDMECs (Figure 3B). L-selectin, a cell adhesion molecule expressed on neutrophils, serves as a master regulator of neutrophil adhesion (30). We next examined whether LRG1 exerts its function through mediating the expression of L-selectin on neutrophils. Indeed, immunoblots showed a significant increase in L-selectin expression in dHL-60 cells subjected to 24-hour treatment with rhLRG1 (Figure 3C). Consistent with this, flow cytometry revealed a marked increase of the median of fluorescence intensity (MFI) in dHL-60 following rhLRG1 treatment (Figure 3E and S2). However, rhLRG1 did not affect the expression of endothelial adhesion molecules including ICAM-1, VCAM-1, P-selectin and E-Selectin (Figure S3). Together, these data show that LRG1 promotes neutrophil adhesion, at least partially, by regulating the expression of L-selectin on neutrophils.

### **LRG1 promotes epithelial cell proliferation and EMT**

Besides inflammation, re-epithelialization is essential to prompt wound repair. It is achieved by orchestrated migration and proliferation of epithelial cells adjacent to the wound (31). H&E analysis revealed delayed re-epithelialization in day-four wounds of *Lrg1*<sup>-/-</sup> mice (Figure 4A). Although the denuded surface is completely covered by newly formed epithelium five days following injury, the reconstituted epidermis is significantly thinner in *Lrg1*<sup>-/-</sup> mice as compared to that in wild-type controls (Figure 4B). It was previously reported that exogenous LRG1 promotes keratinocyte migration (22). Similarly, we showed that LRG1-overexpressing HaCaT cells migrated much faster as compared to control plasmid transfected cells, whereas the migration ability of the LRG1 siRNA-treated HaCaT was significantly compromised (Figure 4C). Activation of the partial epithelial to mesenchymal transition (EMT) has been reported to drive keratinocyte migration (32). Our study demonstrated that rhLRG1 was able to cause a significant induction of key EMT markers, such as fibronectin (FN1) and N-

Cadherin (N-Cad) (Figure 4D). To define LRG1's role in re-epithelialization further, we examined the keratinocyte proliferation as indicated by immunofluorescence staining with Ki67 in day-three wounds of *Lrg1*<sup>-/-</sup> and wild-type control mice. Our study revealed a substantial reduction in the percentage of Ki67-positive keratinocytes at the wound edge of *Lrg1*<sup>-/-</sup> mice (Figure 4E). Consistent with this observation, the number of viable LRG1-overexpressing HaCaT cells was significantly higher than control cells, and HaCaT cells subjected to siRNA-mediated LRG1 knockdown showed reduced viability compared to control siRNA-treated HaCaT (Figure 4F). This observation was supported by a marked increase in cell proliferation marker, Cyclin D1, in rhLRG1-treated HaCaT (Figure 4G). Together, these data suggest that LRG1 facilitates re-epithelialization by promoting keratinocyte proliferation and migration.

### **LRG1 modulates dermal angiogenesis**

Our previous study demonstrated an essential role of LRG1 in pathological neovascularization in the eye (11), and angiogenesis is required for the formation of granulation tissue during wound healing (1). To understand LRG1's role in dermal angiogenesis during wound healing, day-seven wound tissues were subjected to immunofluorescence staining with an EC-specific marker, CD31. Although the total vessel area in the distal part of the skin remain unchanged (Figure S4), there was a significant reduction in total vessel area in the wound bed of *Lrg1*<sup>-/-</sup> mice (Figure 5A). In line with the observations in macrovascular HUVECs (11), rhLRG1 was able to induce HDMEC proliferation as visualised by Ki67 staining (Figure 5B) and the ability of HDMECs to form tube-like structure in Matrigel (Figure 5C). We also showed increased motility of rhLRG1-treated HDMECs (Figure 5D). Mechanistically, we found rhLRG1 significantly stimulated the phosphorylation of pro-angiogenic Smad 1/5 in HDMECs, and blocking of TGF $\beta$  type I receptor activin-like kinase 1 (ALK1) and activin-like kinase 5 (ALK5)

completely abrogated this activation (Figure 5E). These data demonstrate an ALK1/5 dependent pro-angiogenic role of LRG1 in wound healing.

### **LRG1 is highly induced in diabetic mice and humans**

Having established an important role for LRG1 in physiological wound healing, we next examined the association between LRG1 and chronic wound healing in diabetic humans and mice. ELISA analysis revealed a significantly higher LRG1 level in the serum of DFU patients as compared to that in venous ulcer patients (Figure 6A). Consistent with this, we showed that LRG1 expression in ulcer tissues of DFU patients was also significantly higher than that from venous ulcer patients (Figure 6B). To support this observation, wound tissues collected from C57BL/6 mice subjected to STZ-induced type I diabetes were analyzed for the expression of LRG1. As observed in DFU patients, LRG1 levels were significantly higher in wounds of diabetic mice (Figure 6C). Consistently, qRT-PCR analysis revealed a sustained high expression of *Lrg1* transcript in the wound tissue of diabetic mice throughout the wound healing process (Figure 6D). Wound closure was significantly impaired in diabetic mice as compared to that in nondiabetic control (Figure 6E). These data show that in the skin, LRG1 expression is further increased in both humans and mice with diabetes.

### **Deletion of the *Lrg1* gene was beneficial to impaired wound healing in diabetes**

As our data thus far has demonstrated an elevated *Lrg1* transcript level in wounds of both diabetic mice and humans, we investigated whether wound closure in mice with STZ-induced type I diabetes is affected in the absence of *Lrg1*. Unlike what was observed in normoglycemic mice, mice with genetic deletion of *Lrg1* were protected from the diabetes-induced delay in wound closure (Figure 7A). Recent studies highlighted the influence of diabetes on NET formation (8). Considering the role of LRG1 in neutrophil functions and its upregulation at the inflammatory phase of wound healing, we next studied whether LRG1 affects NETosis in mice subjected to STZ-induced type I diabetes. Western blot analysis showed a significant reduction

in the expression of a NET marker H3Cit in day-three wounds of diabetic *Lrg1*<sup>-/-</sup> mice (Figure 7B). To confirm this observation, bone marrow derived neutrophils were isolated from wild-type and *Lrg1*<sup>-/-</sup> mice, and subjected to calcium ionophore (CaI)-induced NETosis. Consistent with the earlier observation, *Lrg1*<sup>-/-</sup> neutrophils were resistant to CaI-induced expression of H3Cit (Figure 7C). Similarly, immunofluorescence staining showed that CaI-induced NETs, as indicated by the presence of H3Cit-positive neutrophils, were significantly reduced in *Lrg1*-deficient neutrophils (Figure 7D). We also showed that *Lrg1*-deficient neutrophils formed fewer NETs in comparison with their wild-type counterparts upon CaI treatments (Figure 7E). To complement this observation, Sytox Green Assay showed that LRG1 supplementation significantly induced the formations of NETs in human peripheral blood neutrophils (Figure 7F). Consistently, immunoblots demonstrated that rhLRG1 significantly induced citrullination of Histone 3 in dHL-60 cells (Figure 7G). Activation of Akt pathway was reported to mediate calcium ionophore-induced NETosis (33). We further showed that LRG1 was able to induce the phosphorylation of Akt in dHL-60 cells and the LRG1-induced expression of H3Cit and Akt phosphorylation were completely abolished in the presence an allosteric Akt inhibitor, MK2206 (Figure 7G). LRG1 was previously reported to signal through TGF $\beta$  type I receptor activin-like kinase 5 (ALK5) in non-ECs (34). To elucidate whether LRG1-induced NETosis and Akt activation is dependent on ALK5, ALK5 was inhibited by SB431542, resulting in a complete abrogation of LRG1-induced phosphorylation of Akt and H3Cit (Figure 7H). Together, our data demonstrate an important role of LRG1 in diabetic wounds and LRG1 exerts its function through mediating NETosis in a TGF $\beta$ /ALK5/Akt-dependent manner.

## **Discussion**

Impaired wound healing and subsequent formation of foot ulcers is one of the most common complications found in patients with diabetes (2). Considering the important role of inflammation in DFU pathophysiology, multiple anti-inflammatory drugs have been developed

but shown limited success (10). LRG1 is a multifunctional protein that was previously linked to neutrophil activation (35), EMT (18) and angiogenesis (11), all of which are essential for effective wound closure. Here, we investigated the role of LRG1 in both physiological and pathological cutaneous wound healing.

Overwhelming evidence indicated the association between LRG1 and various inflammatory and autoimmune conditions (12-15). Infiltrating myeloid cells have been reported to act as the key source of LRG1 in psoriatic skin lesions (13) and remodeling myocardium following infarction (36). In line with these observations, our study revealed that LRG1 is predominantly produced by the wound infiltrating CD11b<sup>+</sup> myeloid cells. Neutrophils are among the first inflammatory cells to reach the wound bed following injury. Both impaired neutrophil function and hyperactive neutrophils have been reported to compromise wound healing (27). Despite being induced during early neutrophil differentiation (37), the role of LRG1 in neutrophil function remains to be elucidated. Our study showed that LRG1 promotes neutrophil adhesion, likely by inducing the expression of neutrophil adhesion molecule, L-selectin. Consistent with this observation, the number of wound-infiltrating neutrophils was significantly reduced in the wound bed of *Lrg1*<sup>-/-</sup> mice. We further showed that wild-type recipients transplanted with *Lrg1*<sup>-/-</sup> BMCs showed a significant delay in wound closure as compared to wild-type recipients receiving wild-type BMCs. On the other hand, wild-type BMCs were sufficient to rescue the delayed wound closure in *Lrg1*<sup>-/-</sup> recipients. These data support the important role of BMDC-derived LRG1 in wound healing.

Re-epithelialization plays an indispensable role in wound healing and it is driven by the proliferation and migration of keratinocytes at the wound edge (31). Previous studies using exogenous LRG1 showed that LRG1 does not affect keratinocyte proliferation as demonstrated by EdU<sup>+</sup> staining (22). Here, we showed reduced number of proliferating keratinocytes as indicated by Ki67 staining at the wound edge of *Lrg1*-deficient mice. The discrepancy between

the two studies is likely due to the use of different cellular markers for proliferating cell detection. Ki67 is a broad cell proliferation marker that is expressed throughout the active cell cycle (G1, S, G2, and M phases) (38), whereas EdU is only incorporated in nascent DNA during the S phase (39). Therefore, EdU may provide partial information regarding the extent of cell proliferation. To support LRG1's role in keratinocyte proliferation, plasmid-mediated LRG1 overexpression and siRNA-mediated LRG1 knockdown treatment significantly affect the viability of keratinocytes *in vitro*. We also demonstrated a promoting role of LRG1 in the expression of cell cycle marker Cyclin D1. These results are in line with previous studies that LRG1 increases proliferation of different epithelial-derived cancer cells, such as colorectal cancer cells (40), pancreatic ductal adenocarcinoma (19), non-small-cell lung cancer cells (41) and gastric cancer cells (42). Consistent with the previous report (22), we showed that LRG1 overexpression and knockdown affect keratinocyte migration. To acquire migratory capacity, quiescent epithelial cells undergo phenotypic changes to gain mesenchymal characteristics (43). Our study discovered that rhLRG1 induces the expression of EMT markers which is consistent with the promoting effect of LRG1 in EMT and colorectal cancer metastasis (44).

The increased metabolic demand of repairing triggers angiogenesis, and failure in forming functional new vessel leads to delayed wound closure (45). Although LRG1 has previously been implicated in ocular (11) and tumor (18) angiogenesis, its role in normal blood vessel formation during wound healing was largely unknown. In this study, we observed reduced blood vessel density in the wound bed of *Lrg1*<sup>-/-</sup> mice. We further showed that LRG1 promotes angiogenesis by mediating HDMEC proliferation, migration and the ability to form tube-like structures. Unlike what was observed in HUVECs (11), both ALK1 and ALK5 are required for LRG1-induced smad1/5/8 phosphorylation in HDMECs, which is not surprising as ALK5 kinase activity is necessary for optimal TGFβ/ALK1 action (46).

Our study showed elevated LRG1 levels in serum and wound tissues of human patients with DFU and diabetic mice, which could be explained, at least partially, by the increased infiltration of immune cells, including neutrophils and macrophages, in diabetic wounds (23, 47). While neutrophils are beneficial to normal wound repair, excessive neutrophil infiltration and NET formation are critical culprits in chronic inflammation and delayed wound closure in diabetes(8). Mechanistically, NETosis could be triggered in a NADPH oxidase (NOX)-dependent and independent manner (33). Our study showed that there was a reduced NETosis in *Lrg1*<sup>-/-</sup> mice and *Lrg1*<sup>-/-</sup>-neutrophils are resistant to calcium ionophore-induced NOX-independent NETosis. Akt is essential for NOX-independent NETosis (33, 48). Furthermore, we demonstrated that LRG1-mediated NETs formation is dependent on activation of the Akt pathway through TGFβ type I receptor, ALK5, which is in agreement with LRG1 mediated TGFβ signaling in ECs (11), fibroblasts (34), glioma cells (49) and T helper 17 cells (50). We further demonstrated that *Lrg1*<sup>-/-</sup> mice are resistant to diabetes-induced delay in wound closure, especially during the inflammatory phase which is likely due to its role in NETosis. It is worth highlighting that global *Lrg1*<sup>-/-</sup> mice were used in this study whereas prompt wound healing is achieved by collaborative interactions between multiple types of cells present in the wound microenvironment (1). Although BMT and *in vitro* experiments demonstrated paracrine role of BMDC-derived LRG1 on other cell types, it remains to be elucidated whether EC and keratinocyte-derived LRG1 plays paracrine or autocrine functions on inflammation, re-epithelialization and angiogenesis. To address these questions, we are now generating cell-specific knockout mice.

In conclusion, we define here a complex but critical role of LRG1 in normal and diabetic wound healing. *Lrg1* deficiency leads to a significant delay in normal wound healing as a consequence of impaired inflammation, re-epithelialization and angiogenesis. On the other hand, there is a reduced NETosis in diabetic mice with ablation of *Lrg1*, which protects *Lrg1*<sup>-/-</sup> from the

diabetes-induced delay in wound healing. Targeting LRG1 may represent an attractive strategy to suppress excessive NETosis, therefore, accelerating wound closure in diabetic patients.

### **Acknowledgement**

We would like to thank John Greenwood and Stephen Moss for providing *Lrg1*<sup>-/-</sup> mice, and David Becker for his advice on histology analysis. This work was supported by Singapore National Medical Research Council Cooperative Basic Research Grant (CBRG) and Singapore Biomedical Research Council-SPF grant (SIPRAD)

### **Author Contributions**

C.L. designed the study, performed experiments, analyzed data, and wrote the manuscript. and M.H.Y.T., S.L.T.P designed and performed experiments and discussed data. M.L.L, H.M.T. performed experiments. S.T., R.C., H.W.H, W.H. contributed to discussion, and reviewed and edited manuscript. X.W. conceived the project, designed the study and wrote the manuscript.

### **Prior Presentation**

Portions of this study were presented at the 3rd Singapore International Conference on Skin Research, Singapore, 2018

### **Data and Resource Availability**

X.W. is the guarantor of this work and, as such, had full access to all the data in the study and takes responsibility for the integrity of the data and the accuracy of the data analysis. Complete datasets generated and analyzed during the current study are available from X.W. upon request.

## References (50)

1. Gurtner GC, Werner S, Barrandon Y, and Longaker MT. Wound repair and regeneration. *Nature*. 2008;453(7193):314-21.
2. Armstrong DG, Boulton AJM, and Bus SA. Diabetic Foot Ulcers and Their Recurrence. *New England Journal of Medicine*. 2017;376(24):2367-75.
3. Morbach S, Furchert H, Groblinghoff U, Hoffmeier H, Kersten K, Klauke GT, et al. Long-Term Prognosis of Diabetic Foot Patients and Their Limbs. *Diabetes Care*. 2012;35(10):2021-7.
4. Gregg EW, Li Y, Wang J, Burrows NR, Ali MK, Rolka D, et al. Changes in diabetes-related complications in the United States, 1990-2010. *N Engl J Med*. 2014;370(16):1514-23.
5. Wild S, Roglic G, Green A, Sicree R, and King H. Global Prevalence of Diabetes. *Diabetes Care*. 2004;27(5):1047.
6. Falanga V. Wound healing and its impairment in the diabetic foot. *The Lancet*. 2005;366(9498):1736-43.
7. Diegelmann RF, and Evans MC. Wound healing: an overview of acute, fibrotic and delayed healing. *Front Biosci*. 2004;9:283-9.
8. Wong SL, Demers M, Martinod K, Gallant M, Wang Y, Goldfine AB, et al. Diabetes primes neutrophils to undergo NETosis, which impairs wound healing. *Nature Medicine*. 2015;21(7):815-9.
9. Rosique RG, Rosique MJ, and Farina Junior JA. Curbing Inflammation in Skin Wound Healing: A Review. *International journal of inflammation*. 2015;2015:316235.
10. Patel S, Srivastava S, Singh MR, and Singh D. Mechanistic insight into diabetic wounds: Pathogenesis, molecular targets and treatment strategies to pace wound healing. *Biomedicine & Pharmacotherapy*. 2019;112:108615.
11. Wang X, Abraham S, McKenzie JAG, Jeffs N, Swire M, Tripathi VB, et al. LRG1 promotes angiogenesis by modulating endothelial TGF- $\beta$  signalling. *Nature*. 2013;499(7458):306-11.
12. Shimizu M, Inoue N, Mizuta M, Nakagishi Y, and Yachie A. Serum Leucine-Rich alpha2-Glycoprotein as a Biomarker for Monitoring Disease Activity in Patients with Systemic Juvenile Idiopathic Arthritis. *J Immunol Res*. 2019;2019:3140204.
13. Nakajima H, Serada S, Fujimoto M, Naka T, and Sano S. Leucine-rich alpha-2 glycoprotein is an innovative biomarker for psoriasis. *J Dermatol Sci*. 2017;86(2):170-4.
14. Shinzaki S, Matsuoka K, Iijima H, Mizuno S, Serada S, Fujimoto M, et al. Leucine-rich Alpha-2 Glycoprotein is a Serum Biomarker of Mucosal Healing in Ulcerative Colitis. *J Crohns Colitis*. 2017;11(1):84-91.
15. Honda H, Fujimoto M, Miyamoto S, Ishikawa N, Serada S, Hattori N, et al. Sputum Leucine-Rich Alpha-2 Glycoprotein as a Marker of Airway Inflammation in Asthma. *PLoS One*. 2016;11(9):e0162672.
16. Yamamoto M, Takahashi T, Serada S, Sugase T, Tanaka K, Miyazaki Y, et al. Overexpression of leucine-rich alpha2-glycoprotein-1 is a prognostic marker and enhances tumor migration in gastric cancer. *Cancer Sci*. 2017;108(10):2052-60.
17. Sng MK, Chan JSK, Teo Z, Phua T, Tan EHP, Wee JWK, et al. Selective deletion of PPARbeta/delta in fibroblasts causes dermal fibrosis by attenuated LRG1 expression. *Cell Discov*. 2018;4:15.

18. Zhang J, Zhu L, Fang J, Ge Z, and Li X. LRG1 modulates epithelial-mesenchymal transition and angiogenesis in colorectal cancer via HIF-1 $\alpha$  activation. *J Exp Clin Cancer Res.* 2016;35:29-.
19. Xie Z-B, Zhang Y-F, Jin C, Mao Y-S, and Fu D-L. LRG-1 promotes pancreatic cancer growth and metastasis via modulation of the EGFR/p38 signaling. *J Exp Clin Cancer Res.* 2019;38(1):75-.
20. Pek SL, Tavintharan S, Wang X, Lim SC, Woon K, Yeoh LY, et al. Elevation of a novel angiogenic factor, leucine-rich-alpha2-glycoprotein (LRG1), is associated with arterial stiffness, endothelial dysfunction, and peripheral arterial disease in patients with type 2 diabetes. *J Clin Endocrinol Metab.* 2015;100(4):1586-93.
21. Pourghaderi P, Yuquimpo K, Sukpraprut-Braaten S, and Waggoner D. Retrospective Clinical Study of Lower Extremity Amputation in Patients with Diabetes Mellitus and Peripheral Arterial Disease: Predictors of Postoperative Outcomes. *J Am Coll Surgeons.* 2017;225(4):S144-S.
22. Gao Y, Xie Z, Ho C, Wang J, Li Q, Zhang Y, et al. LRG1 Promotes Keratinocyte Migration and Wound Repair through Regulation of HIF-1 $\alpha$  Stability. *J Invest Dermatol.* 2020;140(2):455-64.e8.
23. Lan C-CE, Wu C-S, Huang S-M, Wu IH, and Chen G-S. High-glucose environment enhanced oxidative stress and increased interleukin-8 secretion from keratinocytes: new insights into impaired diabetic wound healing. *Diabetes.* 2013;62(7):2530-8.
24. Kayal RA, Tsatsas D, Bauer MA, Allen B, Al-Sebaei MO, Kakar S, et al. Diminished bone formation during diabetic fracture healing is related to the premature resorption of cartilage associated with increased osteoclast activity. *J Bone Miner Res.* 2007;22(4):560-8.
25. Kuhns DB, Priel DAL, Chu J, and Zarembler KA. Isolation and Functional Analysis of Human Neutrophils. *Curr Protoc Immunol.* 2015;111:7.23.1-7.16.
26. Mócsai A, Zhang H, Jakus Zn, Kitaura J, Kawakami T, and Lowell CA. G-protein-coupled receptor signaling in Syk-deficient neutrophils and mast cells. *Blood.* 2003;101(10):4155-63.
27. Wang J. Neutrophils in tissue injury and repair. *Cell Tissue Res.* 2018;371(3):531-9.
28. Koh TJ, and DiPietro LA. Inflammation and wound healing: the role of the macrophage. *Expert Rev Mol Med.* 2011;13:e23.
29. Muller WA. Getting leukocytes to the site of inflammation. *Vet Pathol.* 2013;50(1):7-22.
30. Nagaoka T, Kaburagi Y, Hamaguchi Y, Hasegawa M, Takehara K, Steeber DA, et al. Delayed wound healing in the absence of intercellular adhesion molecule-1 or L-selectin expression. *Am J Pathol.* 2000;157(1):237-47.
31. Pastar I, Stojadinovic O, Yin NC, Ramirez H, Nusbaum AG, Sawaya A, et al. Epithelialization in Wound Healing: A Comprehensive Review. *Adv Wound Care (New Rochelle).* 2014;3(7):445-64.
32. Stone RC, Pastar I, Ojeh N, Chen V, Liu S, Garzon KI, et al. Epithelial-mesenchymal transition in tissue repair and fibrosis. *Cell Tissue Res.* 2016;365(3):495-506.
33. Khan MA, and Palaniyar N. Transcriptional firing helps to drive NETosis. *Scientific Reports.* 2017;7(1):41749.
34. Liu C, Lim ST, Teo MHY, Tan MSY, Kulkarni MD, Qiu B, et al. Collaborative Regulation of LRG1 by TGF-beta1 and PPAR-beta/delta Modulates Chronic Pressure Overload-Induced Cardiac Fibrosis. *Circ Heart Fail.* 2019;12(12):e005962.

35. Druhan LJ, Lance A, Li S, Price AE, Emerson JT, Baxter SA, et al. Leucine Rich  $\alpha$ -2 Glycoprotein: A Novel Neutrophil Granule Protein and Modulator of Myelopoiesis. *PLOS ONE*. 2017;12(1):e0170261.
36. Kumagai S, Nakayama H, Fujimoto M, Honda H, Serada S, Ishibashi-Ueda H, et al. Myeloid cell-derived LRG attenuates adverse cardiac remodelling after myocardial infarction. *Cardiovascular Research*. 2015;109(2):272-82.
37. O'Donnell LC, Druhan LJ, and Avalos BR. Molecular characterization and expression analysis of leucine-rich  $\alpha$ 2-glycoprotein, a novel marker of granulocytic differentiation. *J Leukoc Biol*. 2002;72(3):478-85.
38. Gerdes J, Lemke H, Baisch H, Wacker HH, Schwab U, and Stein H. Cell cycle analysis of a cell proliferation-associated human nuclear antigen defined by the monoclonal antibody Ki-67. *J Immunol*. 1984;133(4):1710-5.
39. Salic A, and Mitchison TJ. A chemical method for fast and sensitive detection of DNA synthesis in vivo. *Proc Natl Acad Sci U S A*. 2008;105(7):2415-20.
40. Zhou Y, Zhang X, Zhang J, Fang J, Ge Z, and Li X. LRG1 promotes proliferation and inhibits apoptosis in colorectal cancer cells via RUNX1 activation. *PloS one*. 2017;12(4):e0175122-e.
41. Li Z, Zeng C, Nong Q, Long F, Liu J, Mu Z, et al. Exosomal Leucine-Rich-Alpha2-Glycoprotein 1 Derived from Non-Small-Cell Lung Cancer Cells Promotes Angiogenesis via TGF-beta Signal Pathway. *Mol Ther Oncolytics*. 2019;14:313-22.
42. Yamamoto M, Takahashi T, Serada S, Sugase T, Tanaka K, Miyazaki Y, et al. Overexpression of leucine-rich  $\alpha$ 2-glycoprotein-1 is a prognostic marker and enhances tumor migration in gastric cancer. *Cancer Sci*. 2017;108(10):2052-60.
43. Yan C, Grimm WA, Garner WL, Qin L, Travis T, Tan N, et al. Epithelial to mesenchymal transition in human skin wound healing is induced by tumor necrosis factor-alpha through bone morphogenic protein-2. *Am J Pathol*. 2010;176(5):2247-58.
44. Zhang J, Zhu L, Fang J, Ge Z, and Li X. LRG1 modulates epithelial-mesenchymal transition and angiogenesis in colorectal cancer via HIF-1alpha activation. *J Exp Clin Cancer Res*. 2016;35:29.
45. Okonkwo UA, and DiPietro LA. Diabetes and Wound Angiogenesis. *Int J Mol Sci*. 2017;18(7):1419.
46. Goumans MJ, Valdimarsdottir G, Itoh S, Lebrin F, Larsson J, Mummery C, et al. Activin receptor-like kinase (ALK)1 is an antagonistic mediator of lateral TGFbeta/ALK5 signaling. *Mol Cell*. 2003;12(4):817-28.
47. Loots MA, Lamme EN, Zeegelaar J, Mekkes JR, Bos JD, and Middelkoop E. Differences in cellular infiltrate and extracellular matrix of chronic diabetic and venous ulcers versus acute wounds. *J Invest Dermatol*. 1998;111(5):850-7.
48. Khan MA, and Palaniyar N. Transcriptional firing helps to drive NETosis. *Scientific reports*. 2017;7:41749-.
49. Zhong D, He G, Zhao S, Li J, Lang Y, Ye W, et al. LRG1 modulates invasion and migration of glioma cell lines through TGF- $\beta$  signaling pathway. *Acta Histochemica*. 2015;117(6):551-8.
50. Urushima H, Fujimoto M, Mishima T, Ohkawara T, Honda H, Lee H, et al. Leucine-rich  $\alpha$  2 glycoprotein promotes Th17 differentiation and collagen-induced arthritis in mice through enhancement of TGF- $\beta$ -Smad2 signaling in naïve helper T cells. *Arthritis Research & Therapy*. 2017;19(1):137.

## FIGURES AND FIGURE LEGENDS

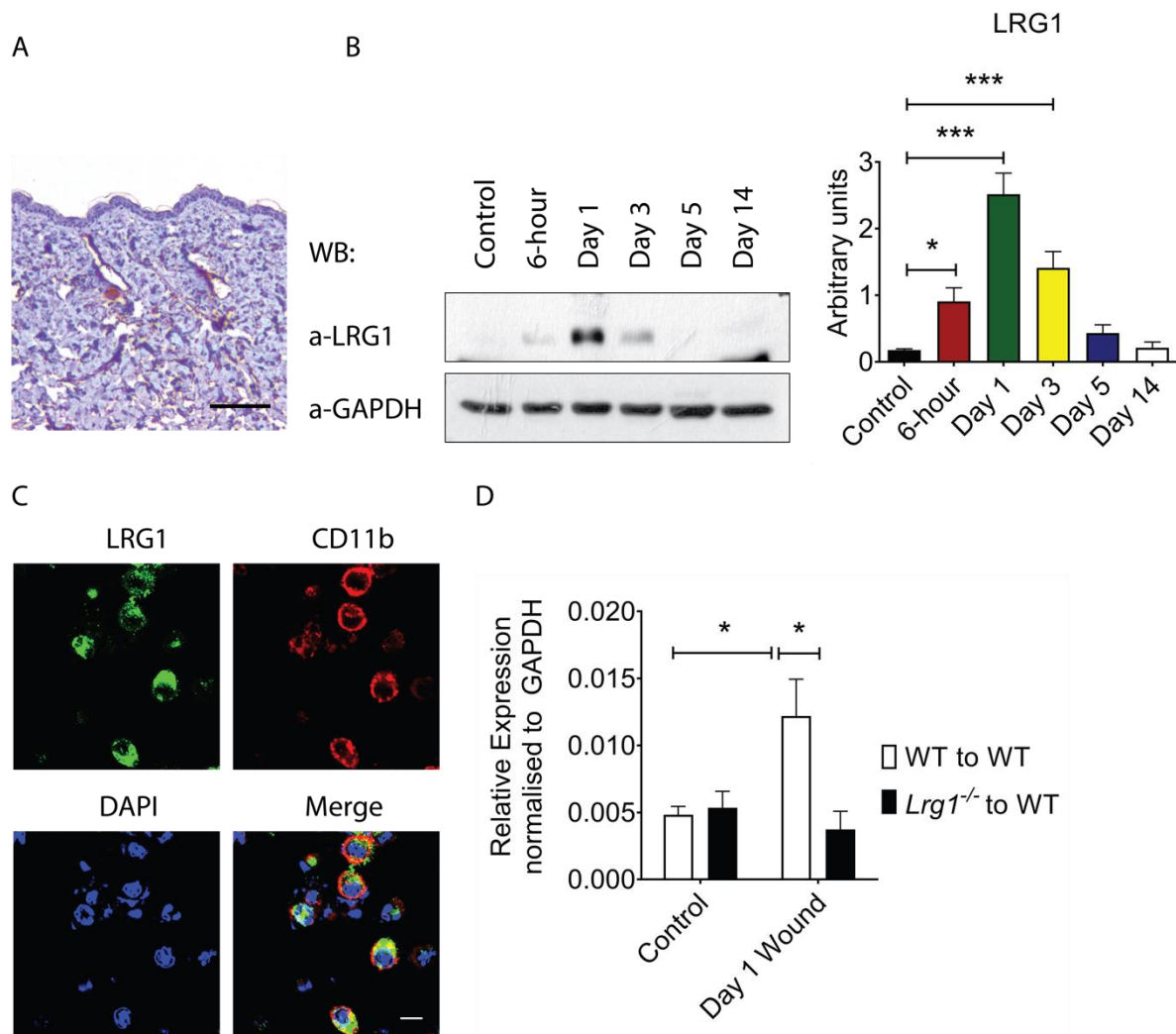


**Figure 1. LRG1 is elevated in cutaneous wounds** (A) Immunohistochemical detection of LRG1 (brown) showed low expression of LRG1 in normal mouse skin. Scale bar: 100 $\mu$ m. (B) Representative western blot (left) and densitometry analysis (right) of wounds harvested at different time points. (C) Immunofluorescence staining detecting LRG1 (green), CD11b (red) or DAPI (4',6-diamidino-2-phenylindole; blue) in day-one mouse wounds. Scale bar: 20 $\mu$ m. (D) qRT-PCR analysis of day-one wounds demonstrated reduced *Lrg1* expression in irradiated wild-type mice with *Lrg1*<sup>-/-</sup> bone marrow cell (BMC) transplantation in comparison with wild-type mice receiving wild-type BMCs. All images are representative; data are represented as mean (95% CI; P) of  $n \geq 5$  mice per group. Significance was determined by one- or two-way ANOVA followed by Tukey multiple comparisons test. \* $P < 0.05$ , \*\*\* $P < 0.001$ . WB indicates western blot.

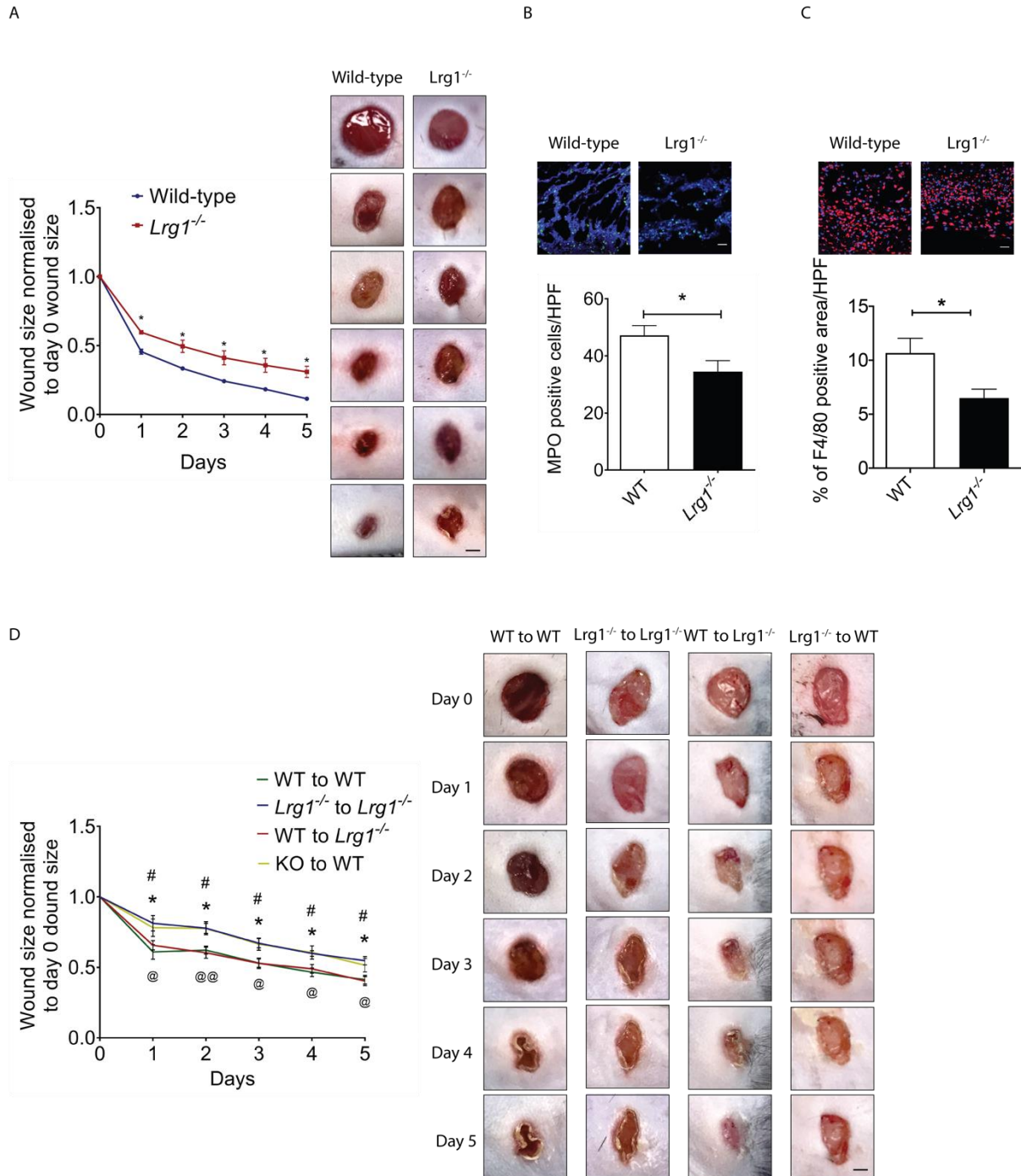


**Figure 2. Absence of *Lrg1* leads to delayed wound healing.** (A) Quantification (left) and representative images (right) of wound size in wild-type and *Lrg1*<sup>-/-</sup> mice revealed a delayed wound closure in the absence of *Lrg1*. \**P*<0.05. Scale bar: 1mm. (B) Representative immunofluorescence staining of MPO (green) and DAPI (blue) (top) and quantification of the presentation of MOP<sup>+</sup> cells (bottom) in day-one wounds of wild-type and *Lrg1*<sup>-/-</sup> mice, five to ten fields per wound were analysed, \**P*<0.05, Scale bar: 30µm. (C) Representative immunofluorescence staining of F4/80 (green) and DAPI (blue) (top) and quantification of F4/80<sup>+</sup> cells (bottom) of in day-five mouse wounds of wild-type and *Lrg1*<sup>-/-</sup> mice, five to ten fields per wound were analyzed, \**P*<0.05. Scale bar: 30µm. (D) Quantification (left) and representative images (right) of wound size in irradiated wild-type (WT) mice receiving BMCs from wild-type mice (WT to WT), irradiated *Lrg1*<sup>-/-</sup> mice receiving BMCs from *Lrg1*<sup>-/-</sup> mice (*Lrg1*<sup>-/-</sup> to *Lrg1*<sup>-/-</sup>), irradiated *Lrg1*<sup>-/-</sup> mice receiving BMCs from wild-type mice (WT to *Lrg1*<sup>-/-</sup>

<sup>-/-</sup>) and irradiated wild-type mice receiving BMCs from *Lrg1*<sup>-/-</sup> mice (*Lrg1*<sup>-/-</sup> to WT). \**P*<0.05: *Lrg1*<sup>-/-</sup> to *Lrg1*<sup>-/-</sup> vs. WT to WT; # *P*<0.05: *Lrg1*<sup>-/-</sup> to WT vs. WT to WT; @ *P*<0.05, @@ *P*<0.01: WT to *Lrg1*<sup>-/-</sup> vs. *Lrg1*<sup>-/-</sup> to *Lrg1*<sup>-/-</sup>. Scale bar: 1mm. All images are representative; data are represented as mean (95% CI; P) of *n* ≥ 6 mice per group. Significance was determined by unpaired, two-tailed Student t-test between wild-type and *Lrg1*<sup>-/-</sup> or wound size at different time points.

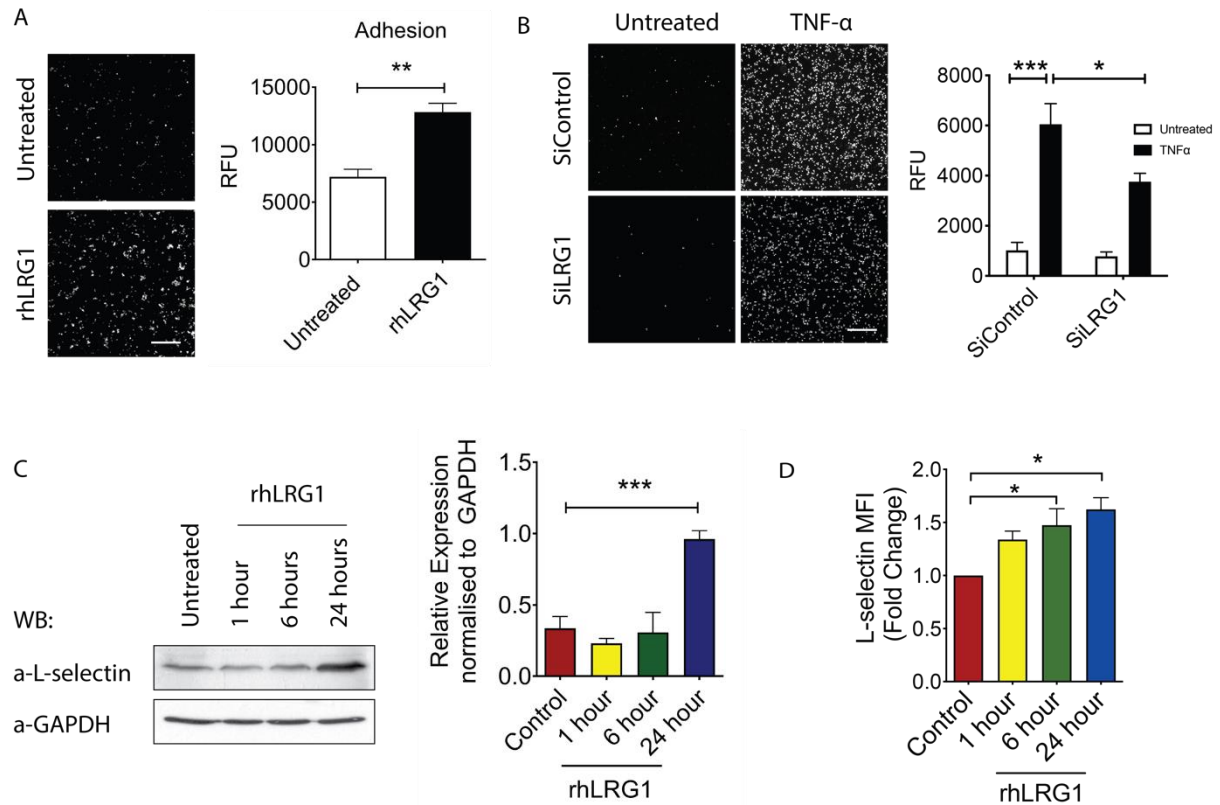


**Figure 3. LRG1 mediates neutrophil adhesion.** (A) Representative images (left) and quantification (right) of neutrophil adhesion assay demonstrated rhLRG1 induced dH60-cells (labeled with CMFDA Dye) adhesion to HDMECs. Scale bar: 200µm. (B) Representative images (left) and quantification (right) of TNFα-induced neutrophil adhesion using hHL-60 cells (labeled with CMFDA Dye) subjected to siRNA-mediated LRG1 knockdown. Scale bar: 200µm. (C) Representative western blot (left) and densitometry analysis (right) of L-selectin and GAPDH in rhLRG1-treated dHL-60 cells at different time points. (D) Quantification of flow cytometry demonstrated an increase in L-sel<sup>High</sup> population following rhLRG1 treatment. All images are representative; data are presented as the mean (95% CI; P) of *n* ≥ 3 independent experiments per group. Significance was determined by one- or two-way ANOVA followed by Tukey multiple comparisons test or unpaired, two-tailed Student t test. \**P*<0.05, \*\**P*<0.01, \*\*\**P*<0.001. WB indicates western blot.

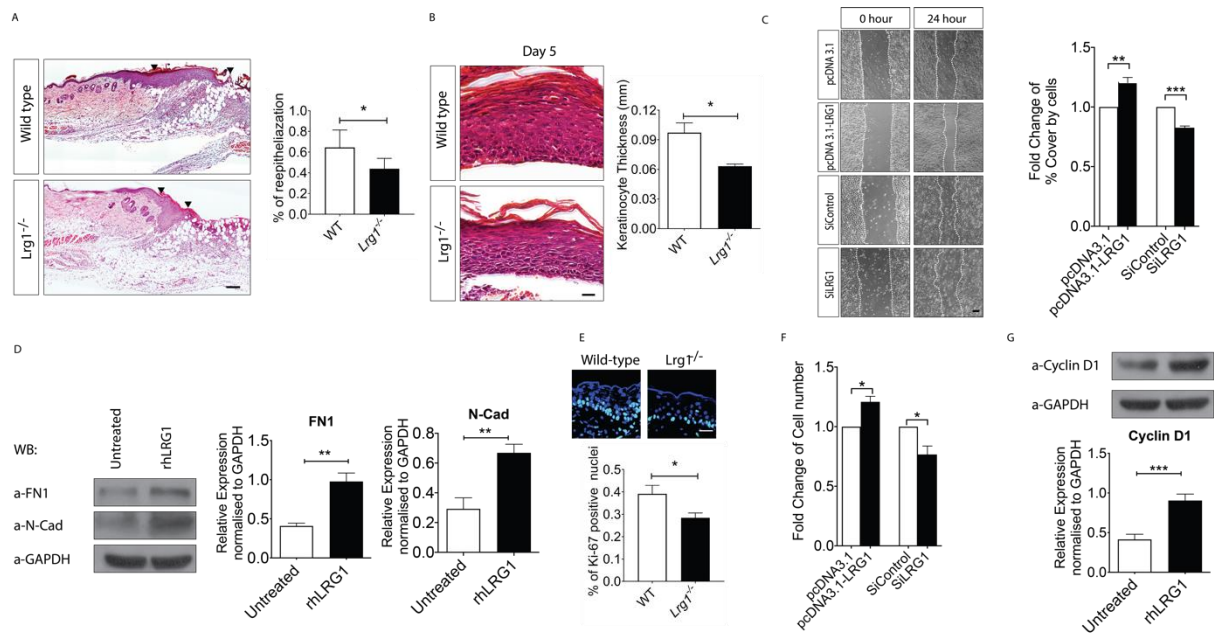
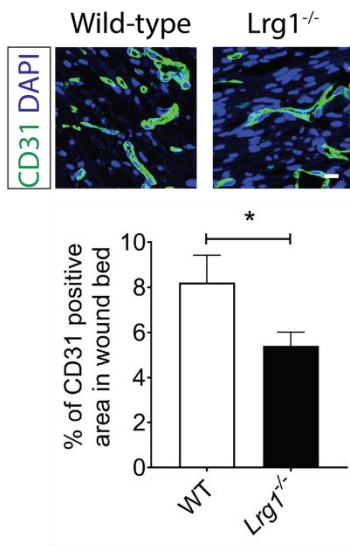
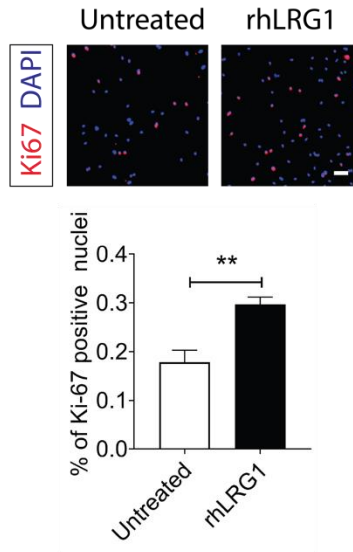


**Figure 4 LRG1 regulates re-epithelialization during wound healing.** (A) Representative H&E staining (left) and quantification of re-epithelialization (right) of day-four wounds of wild-type and *Lrg1*<sup>-/-</sup> mice. Scale bar: 125 $\mu$ m. (B) Representative H&E staining (left) and quantification of epithelium thickness (right) of day-five wounds of wild-type and *Lrg1*<sup>-/-</sup> mice. Scale bar: 25 $\mu$ m. (C) Representative images (left) and quantification of wound gap (right) in scratch wound healing assay. Scale bar: 100 $\mu$ m. (D) Representative western blot (left) and densitometry analysis (right) of fibronectin 1 (FN1), N-cadherin (N-cad) and GAPDH in rhLRG1-treated HaCaT cells. (E) Representative immunofluorescence staining (top) and quantification (bottom) of Ki67 (red) and DAPI (4',6-diamidino-2-phenylindole; blue) in day-three wounds. Scale bar: 30 $\mu$ m. (F) Quantification of viable HaCaT cells in trypan blue exclusion assay (G) Representative western blot (top) and densitometry analysis (bottom) of cyclin D1 and GAPDH in rhLRG1-treated HaCaT cells. All images are representative, and data are represented as mean (95% CI; P) of  $n \geq 6$  mice or  $n \geq 3$  independent experiments per treatment group. Significance was determined by unpaired, two-tailed Student t test. \* $P < 0.05$ , \*\* $P < 0.01$ , \*\*\* $P < 0.001$ . WB indicates western blot.

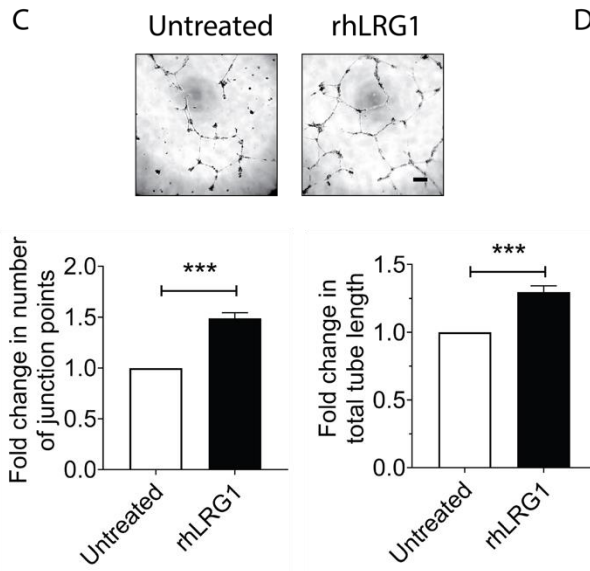
A



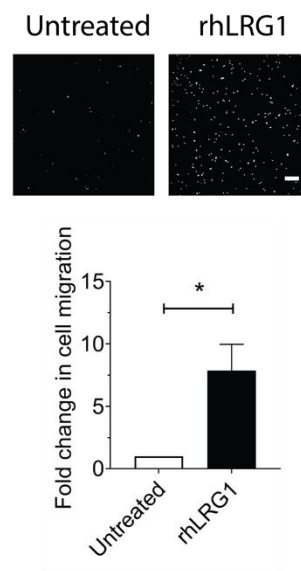
B



C



D



E

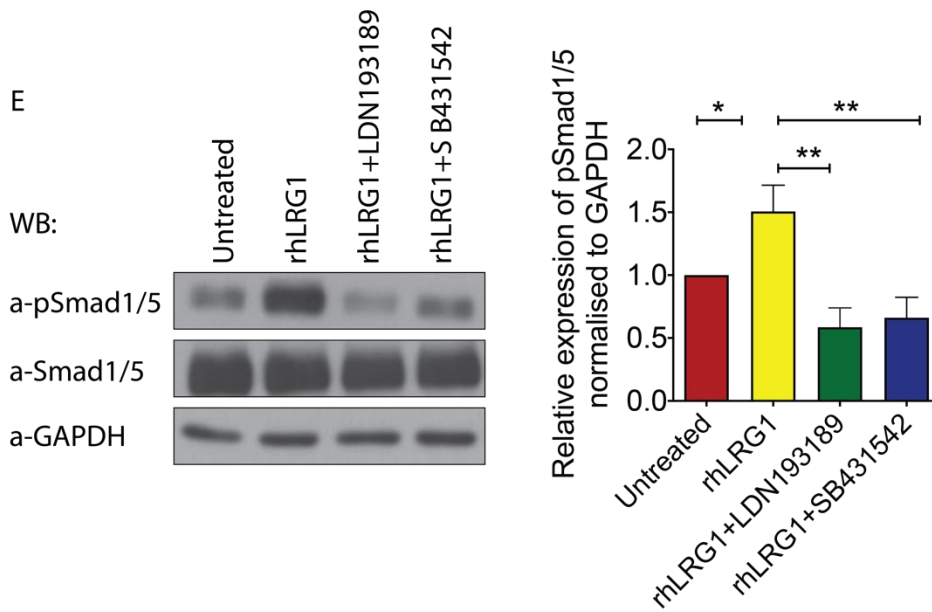


**Figure 5 LRG1 modulates wound angiogenesis during wound healing.** (A) Representative immunofluorescence staining of CD31 (Green) and DAPI (blue) (top) and quantification of vessel density (bottom) in day-seven wounds of wild-type and *Lrg1*<sup>-/-</sup> mice. Scale bar: 15 $\mu$ m. (B) Representative images of immunofluorescence staining detecting Ki67 (red) and DAPI (blue) (top) and quantification of percentage of Ki67<sup>+</sup> cells (bottom) in HDMECs. Scale bar: 50 $\mu$ m. (C) Representative images (left) and quantification (right) of Matrigel tube formation. Scale bar: 125 $\mu$ m. (D) Representative images (top) and quantification (bottom) of Transwell migration assay. Scale bar: 100 $\mu$ m. (E) Representative western blot (left) and densitometry analysis (right) of endothelial TGF $\beta$ /Smad1/5 signaling in HDMECs treated with rhLRG1 in the absence and presence of ALK1 inhibitor (LDN193189) or ALK5 inhibitor (SB431542). All images are representative, and data are represented as mean (95% CI; P) of n  $\geq$  6 mice or n  $\geq$  3 independent experiments per group. Significance was determined by unpaired, two-tailed Student t test. \**P*<0.05, \*\**P*<0.01, \*\*\**P*<0.001. WB indicates western blot.

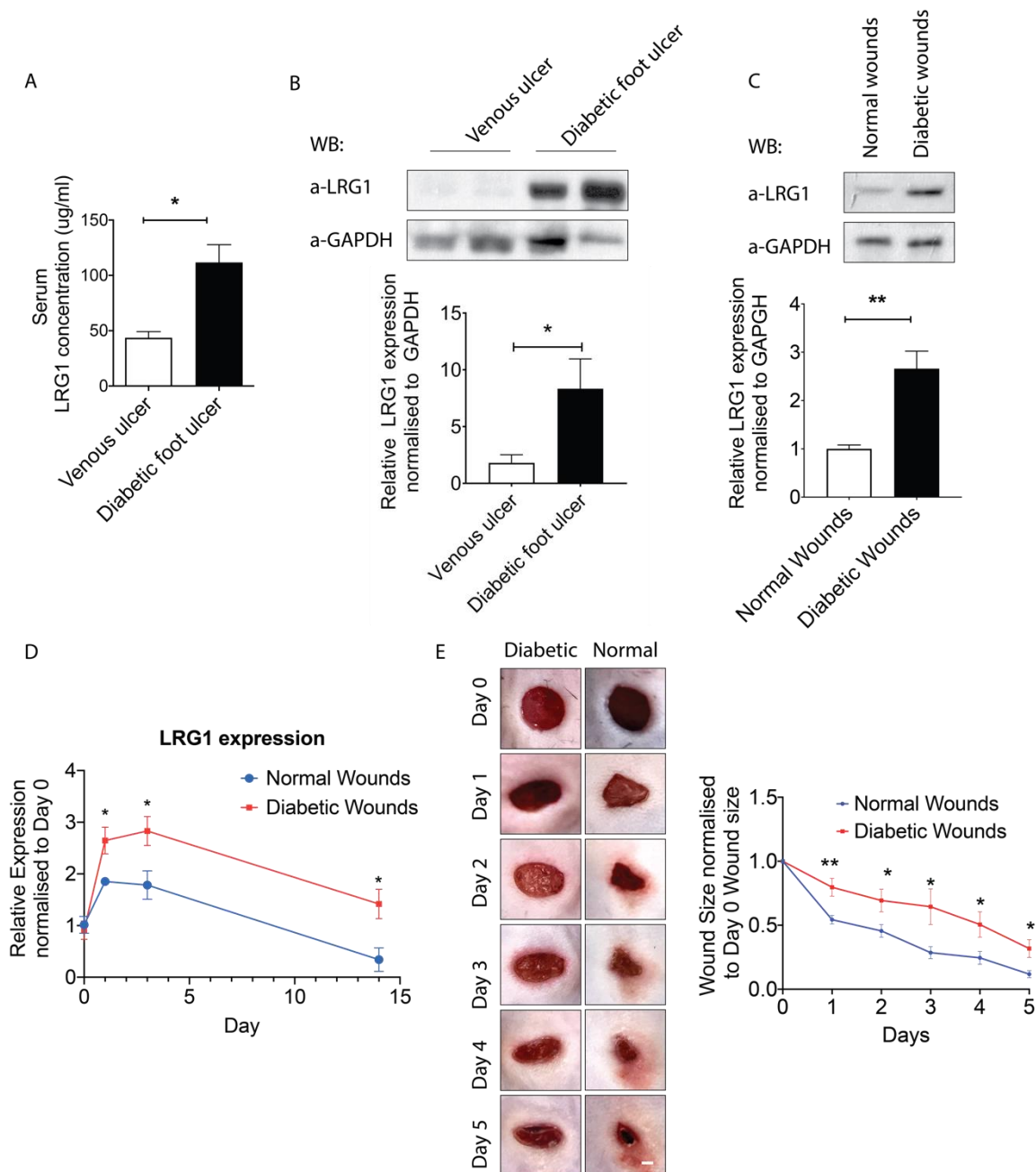


**Figure 6. Elevated LRG1 expression is observed in diabetic humans and mice.** (A) ELISA analysis of LRG1 in serum from patients with venous ulcer and diabetic foot ulcer (DFU) patients. (B) Representative western blot (top) and densitometry analysis (bottom) of LRG1 and GAPDH in human patients with venous ulcer and DFU (C) Representative western blot (top) and densitometry analysis (bottom) of LRG1 and GAPDH in normal and diabetic wounds of C57BL/6 mice. (D) qRT-PCR analysis of normal and diabetic wounds of C57BL/6 mice. (E) Representative images (Left) and quantification (left) of wound size revealed a delayed wound closure in C57BL/6 mice with streptozotocin (STZ)-induced diabetes. Scale bar: 1mm. All images are representative, and data are represented as mean (95% CI; P) of  $n \geq 6$  patients or mice per group. Significance was determined by unpaired, two-tailed Student t test. \* $P < 0.05$ , \*\* $P < 0.01$ , \*\*\* $P < 0.001$ . WB indicates western blot.

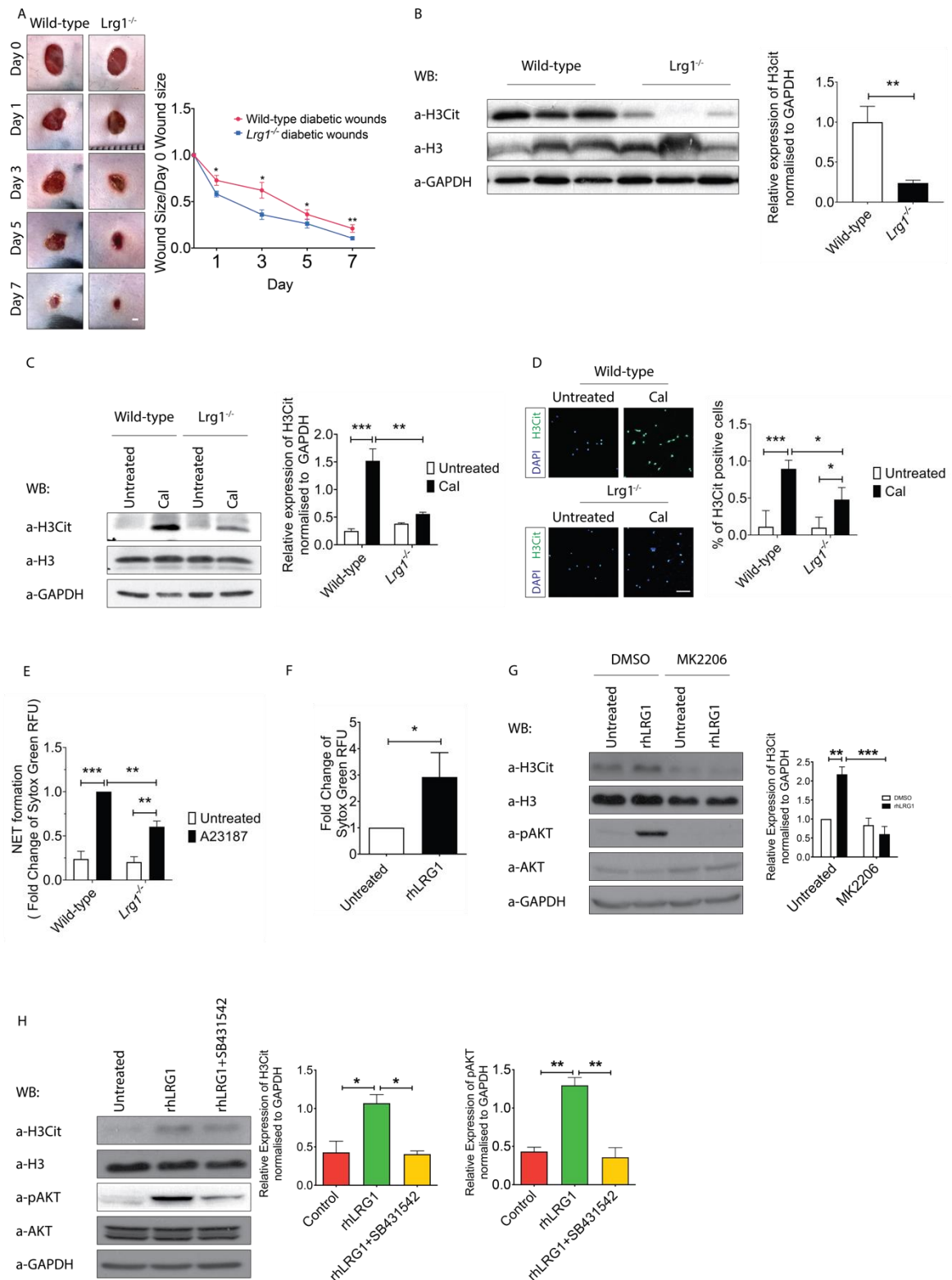


**Figure 7. LRG1 mediates NETosis.** (A) Representative images (left) and quantification (right) of wound size in wild-type and *Lrg1*<sup>-/-</sup> mice with STZ-induced diabetes. Scale bar: 1mm. (B) Representative western blot (left) and densitometry analysis (right) of H3cit, H3 and GAPDH in day-three wounds from wild-type and *Lrg1*<sup>-/-</sup> mice with STZ-induced diabetes. (C) Representative western blot (left) and densitometry analysis (right) of H3cit, H3 and GAPDH

in CaI-treated wild-type and *Lrg1*<sup>-/-</sup> neutrophils. **(D)** Representative immunofluorescence staining detecting H3Cit (Green) and DAPI (blue) (left) and quantification of percentage of H3Cit<sup>+</sup> cells (right) in CaI-treated wild-type and *Lrg1*<sup>-/-</sup> neutrophils. Scale bar: 80µm. **(E)** Sytox Green assay on CaI-treated wild-type and *Lrg1*<sup>-/-</sup> neutrophils. **(F)** Sytox Green assay on CaI-treated dHL-60 cells. **(G)** Representative western blot (left) and densitometry analysis (right) of H3cit, H3, AKT, pAKT (phosphorylated AKT) and GAPDH in rhLRG1 and/or MK2206-treated dHL-60 cells. **(H)** Representative western blot (left) and densitometry analysis (right) of H3cit, H3, AKT, pAKT (phosphorylated AKT) and GAPDH in rhLRG1 with or without SB431542-treated dHL-60 cells. All images are representative, and data are represented as mean (95% CI; P) of n ≥ 6 mice or n ≥ 3 independent experiments per group. Significance was determined by one- or two-way ANOVA followed by Tukey multiple comparisons test or unpaired, two-tailed Student t-test. \**P*<0.05, \*\**P*<0.01, \*\*\**P*<0.00. WB indicates western blot.